Evaluation of ACE-FTS and OSIRIS Satellite retrievals of ozone and nitric acid in the tropical upper troposphere: Application to ozone production efficiency

Matthew Cooper,[1] Randall V. Martin,[1,2] Bastien Sauvage,[3] Chris D. Boone,[4] Kaley A. Walker,[4,5] Peter F. Bernath,[4,6] Chris A. McLinden,[7] Doug A. Degenstein,[8] Andreas Volz-Thomas,[9] and Catherine Wespes[10]

Received 14 September 2010; revised 2 March 2011; accepted 20 March 2011; published 29 June 2011.

[1] We evaluate climatologies of upper tropospheric ozone and nitric acid retrieved from two satellite instruments (ACE-FTS and OSIRIS) with long-term in situ measurements from aircraft (MOZAIC, CR-AVE, PRE-AVE, PEM Tropics, and TC4) and ozonesondes. A global chemical transport model (GEOS-Chem) is used to guide the evaluation and to relate sparse in situ measurements with the satellite retrievals. Both satellite retrievals generally reproduce broad ozone features in the upper troposphere such as summer enhancements in the northern subtropics and larger concentrations over the tropical Atlantic versus the tropical Pacific. These comparisons indicate biases in annual, tropical mean ozone concentrations from both ACE-FTS (10–13%) and OSIRIS (5%) relative to aircraft and ozonesonde observations. More uncertain evidence suggests that nitric acid from ACE-FTS has a positive mean bias of 15%. We demonstrate that an upper limit on the ozone production efficiency in the upper troposphere can be determined using ACE-FTS satellite measurements of O_3 and HNO_3. The resulting value of 196 (+34, −61) mol/mol is in broad agreement with model simulations. Higher OPE values inferred from ACE-FTS over the tropical Pacific (249 (+21, −68) mol/mol) than the tropical Atlantic (146 (+16, −41) mol/mol) reflect increasing ozone production efficiency with decreasing pollution. This analysis indicates a new capability of satellite observations to provide insight into ozone production in the tropical troposphere.

Citation: Cooper, M., R. V. Martin, B. Sauvage, C. D. Boone, K. A. Walker, P. F. Bernath, C. A. McLinden, D. A. Degenstein, A. Volz-Thomas, and C. Wespes (2011), Evaluation of ACE-FTS and OSIRIS Satellite retrievals of ozone and nitric acid in the tropical upper troposphere: Application to ozone production efficiency, *J. Geophys. Res.*, *116*, D12306, doi:10.1029/2010JD015056.

1. Introduction

[2] Ozone (O_3) in the tropical troposphere is a key component in atmospheric oxidation processes and has a large radiative forcing of climate [*Lacis et al.*, 1990; *Thompson*, 1992]. Ozone production in the tropical troposphere is controlled by the supply of nitrogen oxides (NO_x = NO + NO_2) whose main sink is oxidation to nitric acid (HNO_3) [*Murphy et al.*, 1993; *Jacob et al.*, 1996]. Scientific understanding of upper tropospheric ozone is inhibited by sparse measurements in time and space. Well validated satellite observations of HNO_3 and O_3 in the upper troposphere could improve scientific understanding of ozone production and its impact on climate.

[3] Current understanding of upper tropospheric ozone involves a complex interaction of dynamics and photochemical production [*Liu et al.*, 2006; *Nassar et al.*, 2009]. Ozonesonde and aircraft measurements in the upper troposphere indicate low ozone concentrations over marine convective regions and enhanced concentrations over regions of persistent subsidence [*Thompson et al.*, 2003b; *Sauvage*

[1]Department of Physics and Atmospheric Science, Dalhousie University, Halifax, Nova Scotia, Canada.
[2]Harvard-Smithsonian Center for Astrophysics, Cambridge, Massachusetts, USA.
[3]Laboratoire d'Aérologie, CNRS, Université de Toulouse III, Toulouse, France.
[4]Department of Chemistry, University of Waterloo, Waterloo, Ontario, Canada.
[5]Department of Physics, University of Toronto, Toronto, Ontario, Canada.
[6]Department of Chemistry, University of York, York, UK.
[7]Environment Canada, Toronto, Ontario, Canada.
[8]Department of Physics and Engineering Physics, Institute of Space and Atmospheric Science, University of Saskatchewan, Saskatoon, Saskatchewan, Canada.
[9]Institut für Energie und Klimaforschung 8: Troposphäre, Forschungszentrum Jülich, Julich, Germany.
[10]Spectroscopie de l'Atmosphère, Chimie Quantique et Photophysique, Université Libre de Bruxelles, Brussels, Belgium.

0148-0227/11/2010JD015056

et al., 2006]. An outstanding question is the efficiency of ozone production by nitrogen oxides during transport in the upper troposphere. Models predict a high ozone production efficiency in the upper troposphere [*Sauvage et al.*, 2007a], but this result has not been tested with observations. The relationship between O_3 and HNO_3 has been exploited to infer ozone production efficiencies in the lower and middle troposphere [*Trainer et al.*, 1993; *Ryerson et al.*, 1998; *Kleinman et al.*, 2000, 2002; *Hudman et al.*, 2004]. Simultaneous observations of O_3 and HNO_3 from satellites over large spatial scales should offer similar constraints on O_3 production efficiencies in the upper troposphere.

[4] This study focuses on satellite observations of tropical upper tropospheric O_3 and HNO_3 from the Atmospheric Chemistry Experiment Fourier Transform Spectrometer (ACE-FTS) and ozone from the Optical Spectrograph and InfraRed Imaging System (OSIRIS). Previous validation experiments for both instruments have largely focused on either higher latitudes, or on the stratosphere where mixing ratios are higher and satellite retrievals are easier [*Petelina et al.*, 2004; *von Savigny et al.*, 2005; *McLinden et al.*, 2007; *Hegglin et al.*, 2008; *Wolff et al.*, 2008; *Dupuy et al.*, 2009]. No detailed validation of ACE-FTS O_3, ACE-FTS HNO_3 or OSIRIS O_3 with in situ observations throughout the tropical troposphere has been published to date.

[5] The purposes of this study are to (1) evaluate ozone and nitric acid as observed by ACE-FTS and OSIRIS with ozonesonde and aircraft data in the tropical upper troposphere, and (2) examine the information that ACE-FTS provides about the ozone production efficiency. Section 2 describes the satellite and in situ data sets used for this study. Section 3 discusses how a global chemical transport model (GEOS-Chem) is used as a validation tool. Comparisons between the satellite and in situ measurements are displayed and discussed in section 4. The ozone production efficiency is described and is calculated using ACE-FTS measurements in section 5.

2. Data Description

2.1. OSIRIS

[6] OSIRIS was launched on the Odin satellite in 2001 [*Llewellyn et al.*, 2004]. The OSIRIS spectrograph measures scattered sunlight in the limb with wavelengths ranging from ultraviolet to infrared (280 to 800 nm) with 1 nm spectral resolution [*von Savigny et al.*, 2005]. Observations are made between 6 and 60 km with a horizontal resolution of 500 to 1000 km and a vertical resolution of 2 km [*McLinden et al.*, 2007]. The polar, Sun-synchronous, near-terminator orbit of Odin allows for OSIRIS to provide year-round coverage in the tropics, but no coverage in the winter hemisphere due to large solar zenith angles.

[7] This study uses the SaskMART ozone product version 5 for orbits occurring between October 2001 to March 2010 [*Degenstein et al.*, 2009]. Individual sources of error are less than 5% throughout most of the stratosphere, but high altitude clouds may cause larger retrieval errors in the tropical upper troposphere and lower stratosphere [*von Savigny et al.*, 2005]. OSIRIS ozone retrievals have been found to be accurate to within 4–8% in the stratosphere between 15 and 32 km with a total error of 10% [*Petelina et al.*, 2004; *von Savigny et al.*, 2005], however uncertainties increase at lower altitudes, up to 25–30% at 10 km [*McLinden et al.*, 2007].

2.2. ACE-FTS

[8] ACE is a Canadian-led mission on the SCISAT satellite [*Bernath et al.*, 2005]. The main instrument is the ACE-FTS which measures infrared radiation (750 to 4400 cm^{-1}) at a high spectral resolution (0.02 cm^{-1}). ACE-FTS is a solar occultation instrument; the instrument takes a series of measurements while observing the sun rise and set over Earth as it orbits, where each measurement represents a different raypath [*Boone and Bernath*, 2002]. The orbit of SCISAT is such that it observes up to 15 sunrises and sunsets per day, allowing for global coverage over several years. SCISAT's circular low-Earth orbit is optimized for high latitudes and thus provides only medium coverage in the tropics [*Bernath*, 2006]. Retrievals of more than 30 atmospheric species extend from cloud top to 100–150 km altitude with a maximum vertical resolution better than 3 km [*Hegglin et al.*, 2008]. Retrieval version 3 is used here for both ozone and nitric acid measurements spanning January 2004 to August 2010. We exclude all HNO_3 data more than two standard deviations from the median, as a small percentage of the retrievals produced unrealistically high concentrations; this eliminated less than 8% of the data and reduced the bias in section 4. Excluding outliers for O_3 had no significant effect; we retained all O_3 data. ACE-FTS retrievals of NO, NO_2 and CO are also used in this study.

[9] ACE-FTS stratospheric ozone measurements agree to within 10% with ozonesondes and other satellite instruments, including OSIRIS, with ACE-FTS retrievals typically reporting higher values [*Dupuy et al.*, 2009]. These differences increase below 16 km due to increased ozone variability, cloud contamination, and decreased instrument sensitivity [*Dupuy et al.*, 2009]. Comparisons with aircraft measurements between 5 km and the tropopause over Europe indicate a high bias in ACE-FTS O_3 of 18–25% [*Hegglin et al.*, 2008]. ACE-FTS HNO_3 profiles agree with satellite, aircraft, ground-based and balloon observations to within ±1 ppbv in the stratosphere [*Wolff et al.*, 2008].

2.3. In Situ Data

[10] Sources of in situ data used in this study include ozonesondes and aircraft campaigns. Ozonesondes used here are part of the Southern Hemisphere Additional Ozonesondes (SHADOZ, http://croc.gsfc.nasa.gov/shadoz/) network, a group of 16 ozonesonde sites in the southern tropics [*Thompson et al.*, 2003a, 2003b]. Additional ozonesonde data were provided by the World Ozone and Ultraviolet Radiation Data Center (WOUDC, http://www.woudc.org). Given that ozonesondes are launched only 2–3 times a month, seasonal mean values over multiple years provide sufficient observations for accurate climatologies [*Logan*, 1999]. Table 1 lists ozonesonde sites used in this study. Additional ozone and total odd nitrogen ($NO_y = NO_x + HNO_3$ + PAN + other organic nitrates) observations are provided by the Measurement of Ozone and Water Vapor by Airbus In-Service Aircraft (MOZAIC) program [*Marenco*

Table 1. List of Ozonesonde Sites Used

Site	Location	Years Included	Count
American Samoa	170°W/14°S	1998–2008	384
Ascension Island	14°W/8°S	1998–2008	493
Costa Rica	84°W/10°N	2005–2008	167
Fiji	178°E/18°S	1998–2005, 2007–2008	275
Hilo, Hawaii	155°W/19°N	1998–2008	545
Hong Kong	114°E/22°N	2000–2009	403
Huntsville, Alabama	87°W/35°N	1999–2007	110
Irene, South Africa	28°E/26°S	2002–2007	141
Kagoshima	131°E/32°N	1969–2005	257
Kuala Lumpur	101°E/2°N	1998–2007	235
Nairobi	36°E/1°S	1998–2008	472
Natal	35°W/5°S	1998–2008	380
New Delhi	77°E/28°N	1969–1976, 1982–1986, 1994–2009	82
Paramaribo	55°W/6°N	1999–2007	323
Poona, India	73°E/18°N	1969–1976, 1982–1986, 1996–2009	77
La Reunion	55°E/21°S	1998–2008	270
San Cristobal	89°W/1°S	1998–2008	379
Santa Cruz	16°W/28°N	1996, 1999–2003	124
Watukosek, Java	112°E/7°S	1998–2008	257

et al., 1998; *Volz-Thomas et al.*, 2005]. The MOZAIC program places instruments onboard commercial aircraft to measure water vapor, ozone, NO_y and CO at cruising altitudes between 9 and 12 km. Measurement precision is estimated to be 2 ppbv ± 2% or better for each 4 s measurement for tropospheric ozone concentrations, and ozone climatologies produced from MOZAIC observations agree with ozonesondes to within their uncertainties [*Thouret et al.*, 1998a, 1998b]. NO_y measurement precision is given as better than 50 pptv for a 4 s integration time, however the overall statistical error can be up to 200 pptv for measurements in the tropical upper troposphere [*Volz-Thomas et al.*, 2005]. Ozone measurements from 1500 flights in the tropics (20°N–20°S) between 1994 and 2006 and NO_y measurements from 160 flights from 2001 to 2005 are used here.

[11] Measurements of O_3 and HNO_3 from several aircraft campaigns are used in this study. Data from the NASA WB-57F high-altitude research aircraft were collected for the NOAA Pre-Aura Validation Experiment (PRE-AVE) in January and February 2004 and the Costa Rica Aura Validation Experiment (CR-AVE) in February 2006 [*Popp et al.*, 2009]. Additional flights originating in Costa Rica and Panama were part of the Tropical Composition, Cloud and Climate Coupling (TC4) in July and August 2007 [*Toon et al.*, 2010]. HNO_3 measurement accuracy for a 10 s interval is reported as 25% with a precision of 40 pptv or better, and O_3 measurements are accurate to within 5% [*Popp et al.*, 2009]. TC4, CR-AVE and PRE-AVE data are available at the NASA Earth Science Project Office Archives (http://espoarchive.nasa.gov). Measurements across the tropical Pacific were taken by instruments onboard the NASA DC-8 as part of the Pacific Exploratory Mission in the Tropical Pacific (PEM-Tropics) [*Hoell et al.*, 1999; *Raper et al.*, 2001]. Phase A of the mission occurred August–September 1996 while Phase B followed in March–April 1999. HNO_3 measurement accuracy is reported as 30–35% and O_3 measurement accuracy is reported at 3% [*Hoell et al.*, 1999]. PEM-Tropics data are available at the NASA Global Tropospheric Experiment Field Missions archive (http://www-gte.larc.nasa.gov/gte_fld.htm).

2.4. Tropopause Altitude

[12] Knowledge of the tropopause altitude is useful when comparing measurements in the upper troposphere as large vertical gradients may occur in the tropopause region [*Liu et al.*, 2006]. A thermal tropopause is often appropriate in the tropics, while a dynamic tropopause based on potential vorticity may be more appropriate at midlatitudes [*Hoinka*, 1998]. For ACE-FTS we use the combined thermal-dynamic tropopause that is already available as one of the Derived Meteorological Products [*Manney et al.*, 2007]. For OSIRIS, MOZAIC, ozonesondes and GEOS-Chem, we calculate the tropopause as the lowest altitude from either the thermal or dynamic definition. The thermal tropopause is obtained from the NCEP Reanalysis data provided by the NOAA/OAR/ESRL PSD, which defines the tropopause as the lowest level where the temperature lapse rate is less than 2 K/km [*Kalnay et al.*, 1996] (http://www.esrl.noaa.gov/psd). The dynamic tropopause is defined as the lowest level where potential vorticity exceeds 2.5×10^{-6} K m^2 kg^{-1} s^{-1} following *Liu et al.* [2006]. Potential vorticity profiles were obtained from the European Centre for Medium-Range Weather Forecasts (ECMWF) ERA-Interim data, provided by ECMWF. We reject all data within 2 km of the tropopause to account for the satellite vertical resolution and avoid stratospheric air.

3. Using a Model as an Evaluation Tool

[13] Tropospheric ozone concentrations are subject to substantial geophysical variability. As both the ozonesonde and aircraft observation networks have restricted spatial distributions and sampling times, coincident measurements between in situ and satellite data can be infrequent.

[14] A global 3-D model can help bridge the gap between localized in situ measurements and the global coverage provided by the satellite instruments. This study utilizes the GEOS-Chem model which is described in the Appendix. A seasonal mean simulated ozone profile was produced by sampling the GEOS-Chem model at the ozonesonde or MOZAIC flight path locations. These profiles were then compared to simulated seasonal mean ozone profiles over larger domains surrounding the measurement sites. Domain boundaries for comparison of satellite and in situ data were chosen to maximize the area of each region while ensuring that the simulated seasonal mean domain average profile agreed with the locally sampled simulated seasonal mean profiles to within 5 ppbv for all altitudes between 7 and 14 km. This method maximizes the number of satellite observations that fall in each domain while limiting errors due to spatial variations between flight paths, ozonesonde locations and satellite observation locations. This method also allows comparisons to be made using noncoincident measurements by comparing seasonal mean profiles for each region.

[15] The satellite measurements can also be indirectly compared with the in situ observations using a model as a transfer function. This approach is of particular value for comparing short duration aircraft campaigns with satellite observations, as is done here for the evaluation of ACE-FTS HNO_3. GEOS-Chem has been previously used as an

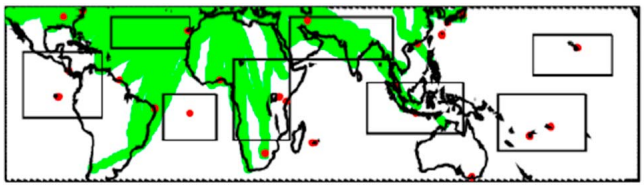

Figure 1. Boxes defining the domains used to calculate seasonal mean ozone profiles. Also displayed are aircraft flight paths (green) and ozonesonde site locations (red).

intermediary step for evaluation of satellite retrievals [*Zhang et al.*, 2010].

4. Evaluation Results

4.1. Ozone Evaluation

[16] Figure 1 shows the eight regions used for our global evaluation of ACE-FTS and OSIRIS measurements. The boundaries of these regions were chosen following the method outlined in section 3. MOZAIC data are used in the boxes over Central Asia, Africa and the North Atlantic, and ozonesondes are used in the Tropical Atlantic (Ascension), Africa (Nairobi), Oceania (Kuala Lumpur, Java) and three Pacific regions (Hilo in North Pacific, San Cristobal and Costa Rica in East Pacific, Fiji and Samoa in South Pacific).

[17] Figure 2 shows seasonal mean ozone profiles and their standard errors within each region. Seasonal mean ozone concentrations from in situ measurements in the upper troposphere range from 30 ppbv over the tropical Pacific in December–February due to persistent deep convection [*Folkins et al.*, 2002] to 70 ppbv over Africa in September–November due to a combination of lightning and biomass burning [*Thompson et al.*, 1996]. The small standard errors indicate sufficient observations to assess bias, with the exception of some ACE-FTS mean profiles that were calculated using a small number of observations. As described in section 3, we estimate the uncertainty in the comparison of point observations from ozonesondes and flight paths with satellite observations over the eight larger domains to be less than 5 ppbv.

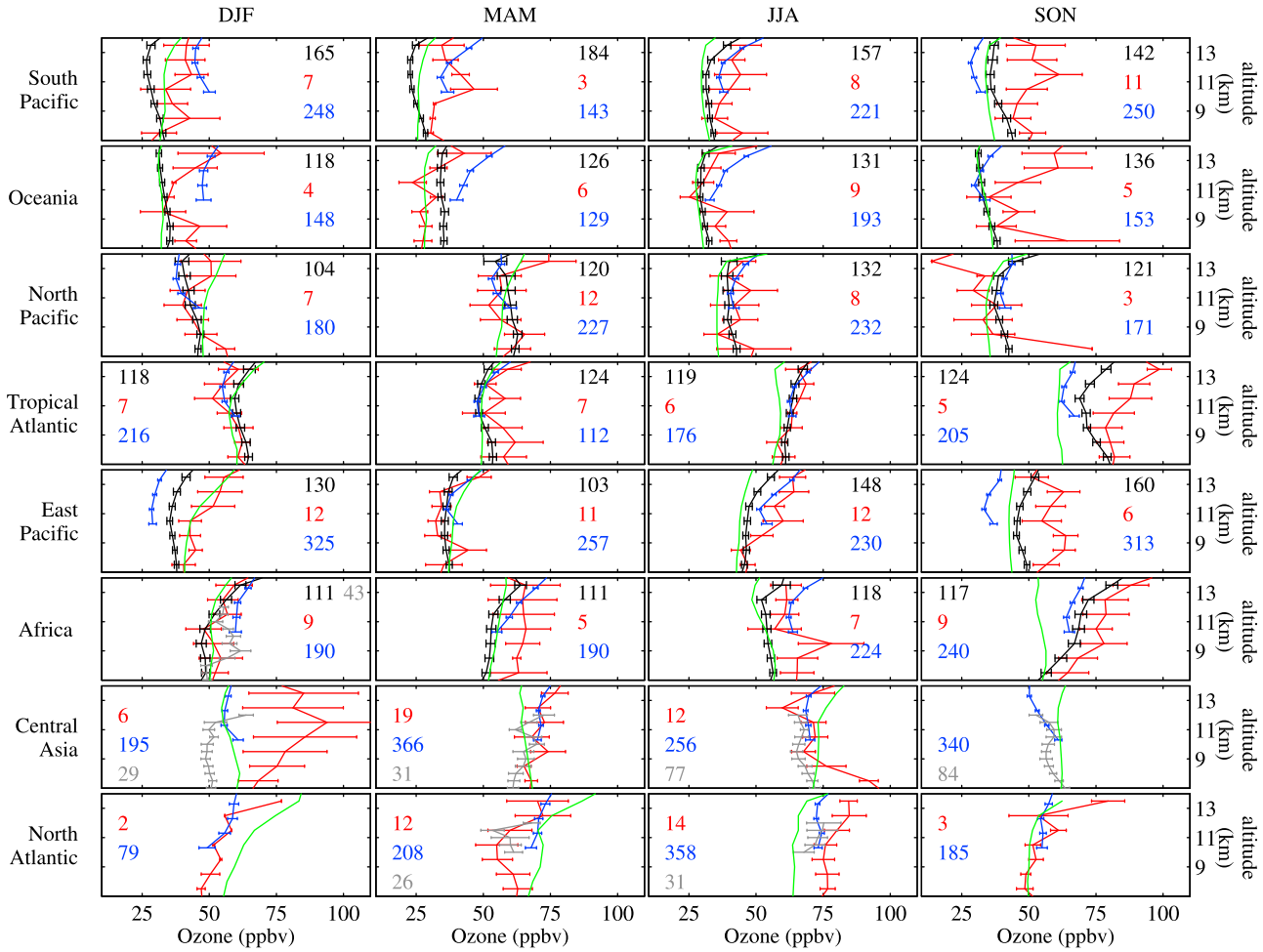

Figure 2. Seasonal mean ozone profiles from GEOS-Chem (green), ozonesondes (black), aircraft (grey), OSIRIS (blue), and ACE-FTS (red). Numbers indicate the number of ozonesonde launches, flight paths, or satellite observations used to calculate the averages. Error bars represent ±1 standard error of the mean. Regions are defined in Figure 1. DJF, December–February; MAM, March–May; JJA, June–August; SON, September–November.

Table 2. Annual Mean Absolute and Percent Differences Between Satellite and in Situ Ozone Profiles

	ACE-FTS – Ozonesondes		ACE-FTS – MOZAIC		OSIRIS – Ozonesondes		OSIRIS – MOZAIC	
Region	ppbv	Percent	ppbv	Percent	ppbv	Percent	ppbv	Percent
South Pacific	12	41	N/A	N/A	8	27	N/A	N/A
Indonesia	4	12	N/A	N/A	7	23	N/A	N/A
Africa	8	14	−4	−7	4	8	4	7
Central Asia	N/A	N/A	10	16	N/A	N/A	3	5
North Atlantic	N/A	N/A	1	2	N/A	N/A	3	4
North Pacific	−1	−2	N/A	N/A	0.1	0.2	N/A	N/A
East Pacific	8	19	N/A	N/A	−3	−7	N/A	N/A
Tropical Atlantic	4	7	N/A	N/A	−3	−4	N/A	N/A
Global	5	13	6	10	2	5	3	5

[18] The agreement between seasonal mean satellite profiles and the in situ observations is variable. In some cases, such as the East Pacific in MAM, the observational data sets agree well. In other cases, such as the East Pacific in DJF, significant differences exist. Regional differences are summarized in Table 2. In the global annual mean, both OSIRIS and ACE-FTS tend to be biased high. OSIRIS ozone concentrations are on average 5% higher (RMSE = 4 ppbv) than the MOZAIC profiles and 5% higher (RMSE = 8 ppbv) than the ozonesondes. This is an improvement compared to the retrieval version 2.1 evaluation in the lower stratosphere by *McLinden et al.* [2007]. Although the relatively lower number of ACE-FTS measurements in each region increases scatter, the ACE-FTS profiles have significant mean biases of 10% versus MOZAIC (RMSE = 18 ppbv) and 13% versus ozonesondes (RMSE = 10 ppbv). This is an improvement compared with previous ACE-FTS validation efforts over Europe, which found a positive bias of 25% in ACE-FTS O_3 in the upper troposphere [*Hegglin et al.*, 2008]. Excluding satellite data outside three standard deviations of the median changed annual mean ozone profiles by less than 3% for OSIRIS and less than 1% for ACE-FTS.

[19] Seasonal mean simulated O_3 profiles from GEOS-Chem generally agree with the in situ observations to within 10 ppbv (mean bias 4% for MOZAIC, 3% for ozonesondes), the most prominent discrepancy is over Central Asia during DJF when the simulated ozone is higher than MOZAIC by

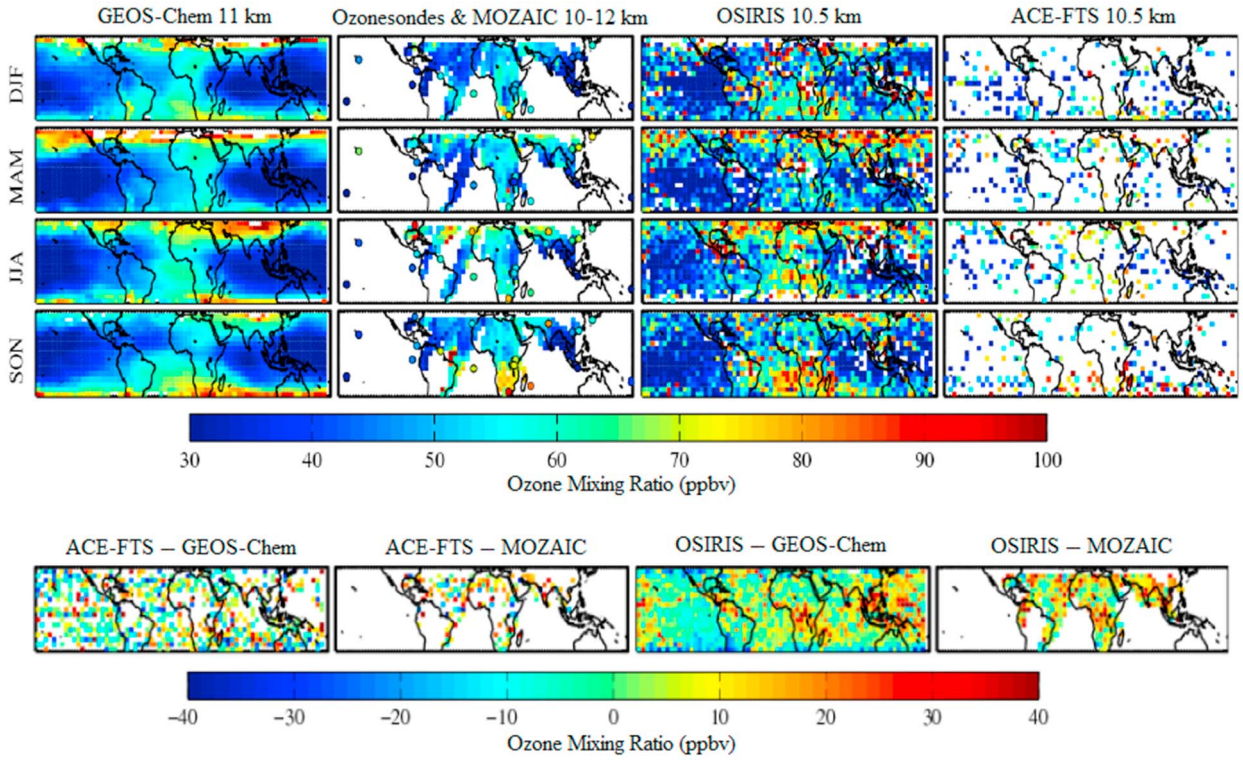

Figure 3. (top) Seasonal mean ozone concentrations from GEOS-Chem, MOZAIC, OSIRIS, and ACE-FTS in the upper troposphere (10–12 km). Circles on MOZAIC maps represent seasonal mean ozonesonde observations. (bottom) Annual mean differences between the satellite, MOZAIC, and GEOS-Chem data sets.

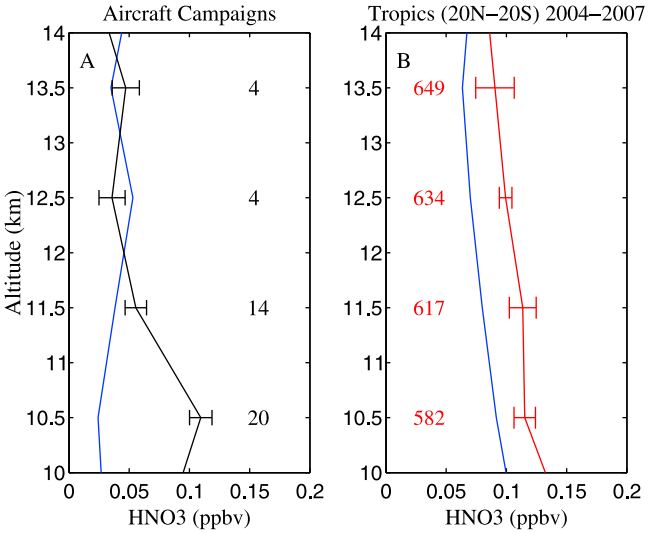

Figure 4. Mean nitric acid (HNO_3) vertical profiles. (a) Aircraft data (black) with GEOS-Chem simulation sampled along the flight path (blue) for CR-AVE, PRE-AVE, and PEM Tropics A and B campaigns. (b) Annual (2004–2007) mean tropical HNO_3 profile from ACE-FTS (red) and GEOS-Chem sampled at the month and location of the ACE-FTS observations (blue). Numbers indicate the number of data points used for comparison.

20%, perhaps reflecting issues in representing stratosphere-troposphere exchange [*Zhang et al.*, 2010].

[20] Figure 3 shows maps of seasonal mean upper tropospheric (10–12 km) ozone concentrations from GEOS-Chem, MOZAIC and both satellite instruments. Ozonesondes listed in Table 1 are also displayed. All maps broadly indicate the wave-one pattern of higher O_3 concentrations over the tropical Atlantic Ocean than the Pacific [*Thompson et al.*, 2003b]. This pattern reflects ozone production from lightning and persistent subsidence over the tropical Atlantic [*Martin et al.*, 2002]. We compare the tropical seasonal mean ozone concentrations from GEOS-Chem and MOZAIC with the seasonal mean concentrations from the satellite retrievals. MOZAIC and GEOS-Chem show good agreement throughout the tropics (r = 0.5, mean bias 7%, RMSE = 11 ppbv) although GEOS-Chem ozone concentrations in the northern subtropics are higher than MOZAIC particularly during March–May. *Zhang et al.* [2010] also found indications of a model overestimation versus ozonesondes at midlatitudes, which may be related to excessive stratospheric influx. Both ACE-FTS and OSIRIS have modest agreement with MOZAIC (r = 0.4, RMSE = 22 ppbv, mean bias 15% for ACE-FTS, r = 0.2, RMSE = 24 ppbv, mean bias 20% for OSIRIS) and GEOS-Chem (r = 0.5, RMSE = 7 ppbv, mean bias 7% for ACE-FTS, r = 0.4, RMSE = 20 ppbv, mean bias 10% for OSIRIS). The differences between the satellites, MOZAIC and GEOS-Chem are also displayed in Figure 3.

4.2. Nitric Acid Evaluation

[21] While SHADOZ and MOZAIC provide sufficient observations for ozone comparisons, a comprehensive set of in situ HNO_3 measurements is not available. Instead, aircraft measurements of HNO_3 from aircraft campaigns (CR-AVE, PRE-AVE, TC4, PEM Tropics) and of NO_y from MOZAIC are used to evaluate GEOS-Chem, which is in turn compared with ACE-FTS HNO_3 retrievals.

[22] Aircraft measurements were used to evaluate GEOS-Chem by sampling the simulation along the flight paths. Figure 4a shows mean HNO_3 concentrations over the four campaigns. Mean HNO_3 concentrations are typically less than 0.1 ppbv throughout the upper troposphere. The average simulated profile shows HNO_3 concentrations that agree with the aircraft measurements above 11.5 km, however the simulated HNO_3 concentrations are 50% lower than the aircraft measurements between 10 and 11.5 km. Direct comparison of ACE-FTS versus aircraft measurements is inhibited by their lack of coincidence during their short campaigns, and by the high HNO_3 variability. For further insight, we compared ACE-FTS to GEOS-Chem by sampling a monthly mean model simulation at the ACE occultation locations in Figure 4b. ACE-FTS measurements are 38% higher than the modeled profile between 10 and 14 km. Some of this difference may be due to large spatial and temporal variations of HNO_3 that are not captured by the model.

[23] MOZAIC total odd nitrogen (NO_y) measurements are also used to evaluate ACE-FTS and GEOS-Chem as HNO_3 can represent up to 50% of NO_y in the tropical troposphere [*Kasibhatla et al.*, 1993; *Folkins et al.*, 2006]. We approximate NO_y as NO + NO_2 + HNO_3, as these species provide the largest contributions to NO_y and are regularly retrieved by ACE-FTS. PAN can provide a significant contribution to NO_y, however it is not regularly retrieved by ACE-FTS. Therefore we exclude regions where simulated PAN represents more than 30% of the total simulated NO_y.

[24] Figure 5 shows maps of annual mean NO_y concentrations in the tropical upper troposphere from MOZAIC, ACE-FTS and GEOS-Chem. The spatial distribution of ACE-FTS and GEOS-Chem NO_y exhibit a wave-1 pattern showing a maximum over Africa and a minimum over the Pacific, similar to that found by *Martin et al.* [2007] for HNO_3. Simulated NO_y concentrations show some similarities in spatial structure with a mean negative bias versus MOZAIC of 9%. The largest discrepancies are found in regions with few MOZAIC flights, such as Southeast Asia. However, both ACE-FTS NO_y and HNO_3 are significantly larger than the simulated values (mean bias 29% for HNO_3, mean bias 23% for NO_y). Adding simulated PAN to the ACE-FTS NO_y would increase the mean bias to 55%. Including data lying outside two standard deviations of the median would increase the mean bias to 50%.

[25] In summary, both the comparisons with CR-AVE and MOZAIC provide evidence of a positive bias in ACE-FTS. The larger spatial and temporal domain of the comparison with MOZAIC yields a more quantitative estimate. Considering the negative bias in the simulated NO_y versus MOZIAC, we find evidence of a positive mean bias in ACE-FTS HNO_3 of 15%. This bias is greater than the error found in stratospheric validations [*Wolff et al.*, 2008], but consistent with the validation over Europe by *Hegglin et al.* [2008]. This evaluation shows improvement in the ACE-FTS version 3 retrievals, especially in the middle troposphere, when compared to previous studies of ACE-FTS

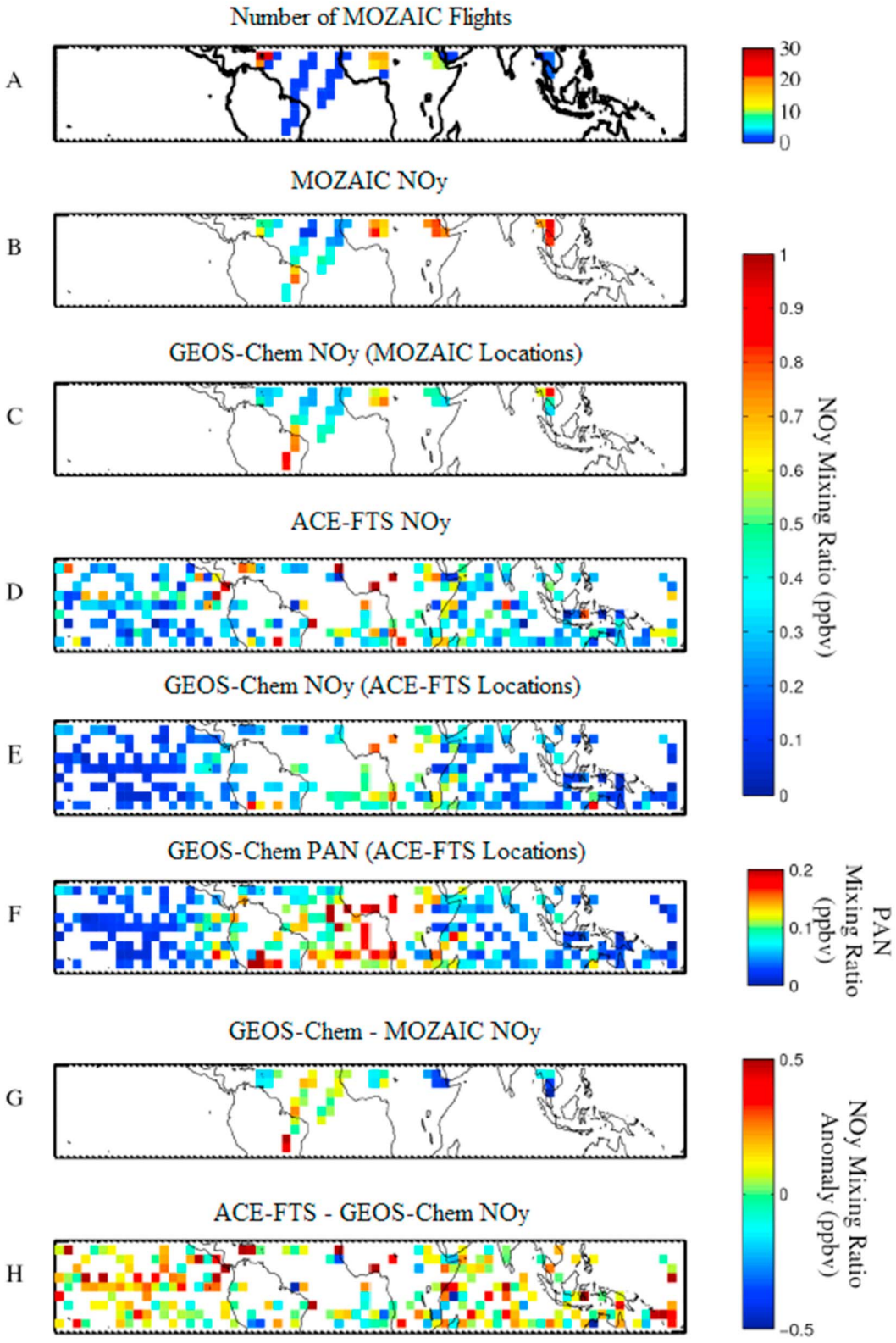

Figure 5. (a) Number of MOZAIC flights where NO_y is measured. Annual mean NO_y concentrations from (b) MOZAIC, (c) GEOS-Chem sampled along MOZAIC flight paths, (d) ACE-FTS, and (e) GEOS-Chem sampled at ACE-FTS locations and months. Data in Figures 5b–5e are excluded in regions where the contribution of PAN to simulated NO_y concentrations exceeds 30%. (f) Annual mean PAN concentrations from GEOS-Chem sampled at ACE-FTS locations and months. Annual mean differences between (g) MOZAIC and GEOS-Chem NO_y, and (h) ACE-FTS and GEOS-Chem NOy.

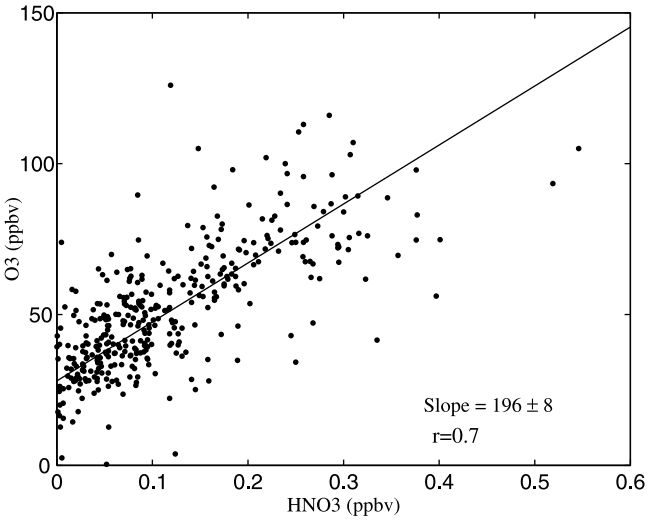

Figure 6. Scatterplot of ACE-FTS O3 versus HNO_3 used to infer ozone production efficiency (OPE) at 11.5 km. Each point represents a monthly mean of ACE-FTS measurements on a 2° latitude by 2.5° longitude grid in the tropics (20°N–20°S). The line of best fit is determined by reduced major-axis linear regression [*Miller and Kahn*, 1962].

version 2.2 versus GEOS-Chem [*Folkins et al.*, 2006]. In the next section, we will use the biases inferred here.

5. Ozone Production Efficiency

5.1. Estimating Ozone Production Efficiency

[26] We go on to develop a method to interpret the ACE-FTS observations for insight into the ozone production efficiency (OPE). OPE can be defined as the number of O_3 molecules produced per NO_x molecule consumed [*Liu et al.*, 1987]. Several studies have calculated OPE using aircraft or surface measurements of O_3 and HNO_3. Near-surface OPE has been found to range from 2 mol/mol in polluted urban regions [*Kleinman et al.*, 2000] to 10 mol/mol in rural areas [*Trainer et al.*, 1993]. These studies show that OPE increases with decreasing NO_x [*Kleinman et al.*, 2002]. OPE is greater in the free troposphere than at the surface due to low NO_x concentrations as well as low humidity and more intense solar radiation [*Sauvage et al.*, 2007a]. *Hudman et al.* [2004] used aircraft observations of a pollution plume crossing the Pacific Ocean to estimate the OPE in the middle troposphere as 53 mol/mol.

[27] ACE-FTS measurements of upper tropospheric O_3 and HNO_3 can be used to estimate OPE. Convective outflow in the upper troposphere contains some initial ozone and NO_x concentration but is depleted of HNO_3 due to its high solubility [*Mari et al.*, 2000]. Ozone is produced in the presence of NO_x during transport until the cycle is broken by oxidation of NO_x to HNO_3. The loss of NO_x is therefore nearly equivalent to HNO_3 production, and the OPE can be inferred by the ratio of O_3 production to HNO_3 production.

$$OPE = \frac{P(O_3)}{L(NO_x)} \approx \frac{\Delta O_3}{\Delta HNO_3} \quad (1)$$

This expression assumes that O_3 and HNO_3 losses are small. The assumption is reasonable in the tropical upper troposphere, given the long lifetimes of O_3 and HNO_3 in this region. However, the lifetime of the O_3 family (O_x) is longer (90 days in GEOS-Chem) than that of HNO_3 scavenging (75 days in GEOS-Chem). This lifetime difference lowers HNO_3 concentrations and causes an overestimation of OPE. For this reason, the OPE calculation presented here should be considered an upper limit.

[28] We tested the method by comparing a GEOS-Chem calculation of OPE based on O_3 and HNO_3 production rates with an estimate of OPE using a scatterplot of annual mean simulated O_3 and HNO_3. OPE calculated from O_3 and HNO_3 production rates is 26% lower than that estimated from O_3 and HNO_3 concentrations, confirming our expectations of an upper limit. Sampling the model at ACE-FTS measurement locations did not change the tropical mean OPE, indicating that the OPE estimate is not sensitive to ACE-FTS sampling. We also tested the sensitivity to dynamics of the OPE estimated from HNO_3 and O_3 concentrations. We estimated the OPE for two different assimilation systems (GEOS-4 and GEOS-5) that use different convective parameterizations, which lead to variations in the height and intensity of convective outflow in the upper troposphere [*Folkins et al.*, 2006; *Wu et al.*, 2007]. The OPE estimates differed by <2%, indicating this method has little sensitivity to dynamics.

[29] We go on to apply our method to the ACE-FTS data. Figure 6 shows a scatterplot of ACE-FTS O_3 and HNO_3 data between 20°N and 20°S at 11.5 km in the tropical upper troposphere. Each point represents an average of ACE-FTS O_3 and HNO_3 over 2° latitude and 2.5° longitude. The

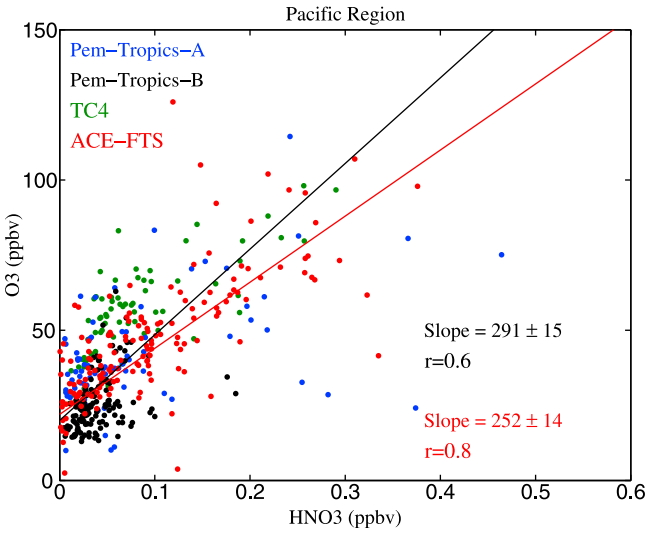

Figure 7. Scatterplot of O_3 versus HNO_3 from ACE-FTS (red), PEM-Tropics A (blue) and B (black), and TC4 (green). Only ACE-FTS measurements over the tropical Pacific (20°N–20°S, 150°E–50°W) at 11.5 km are shown here. The vertical range for aircraft measurements is 8–12 km. Each point represents an average measurement on a 2° latitude by 2.5° longitude grid. Lines of best fit for ACE-FTS (red) and all aircraft (black) data in this region are determined by reduced major-axis linear regression [*Miller and Kahn*, 1962].

Table 3. Regional Ozone Production Efficiency Variations as Estimated From ACE-FTS Measurements[a]

Region	Longitude Range	OPE (mol/mol)	Measurements Count	r (HNO_3 Versus O_3)	Mean CO (ppbv)	δ_p (mol/mol)	δ_r (mol/mol)
Whole Tropics	180°W–180°E	196 (+34, −61)	368	0.71	85	32	7
Tropical Pacific	160°E–130°W	249 (+21, −68)	65	0.80	71	4	19
Tropical Atlantic	50°W–30°E	146 (+16, −41)	62	0.68	100	6	14

[a]Here δp is the error in the OPE estimate due to sensitivity to polluted outflow and δr is the uncertainty in the OPE estimate from the standard error of the reduced major axis regression.

significant correlation (0.7) between the two species implies a single chemical system. As demonstrated in equation (1), OPE is given by the slope of the line of best fit for this plot, which is found by a reduced major axis regression [*Miller and Kahn*, 1962] to be 196 (+34, −61) mol/mol. The method for determining the uncertainty is described below. While 11.5 km was chosen here, OPE estimations from ACE-FTS were consistent between 8 and 12 km. Above 12 km, OPE increases with altitude ($\Delta OPE/\Delta z$ = 40 ± 10 mol/mol/km).

[30] O_3 and HNO_3 measurements from ACE-FTS and aircraft campaigns over the tropical Pacific are shown in Figure 7. Both data sets show similar correlation, and a line fitted to the aircraft data shows a tropical mean in situ OPE estimate that is within 15% of the one found using satellite observations. Differences may reflect different sampling domains. The higher correlation in ACE-FTS (0.8) versus the aircraft data (0.6) could indicate the benefit of sampling a larger air mass.

[31] We explore the horizontal variation in the estimate. Table 3 contains OPE calculated from ACE-FTS separately for the tropical Atlantic and tropical Pacific. OPE values over the tropical Pacific are 67% larger than those over the tropical Atlantic, reflecting increased OPE in less polluted regions. Higher OPE in regions of lower NO_x is consistent with previous OPE calculations [*Liu et al.*, 1987; *Lin et al.*, 1988; *Trainer et al.*, 1993; *Kleinman et al.*, 2002].

[32] We compare the OPE estimate from ACE-FTS with OPE calculated from GEOS-Chem O_3 and HNO_3 production rates, which are shown in Figure 8. OPE ranges from 100 to 150 mol/mol or higher throughout the middle and upper troposphere over the tropical South Atlantic [*Sauvage et al.*, 2007a], and over the tropical Pacific can exceed 200 mol/mol. These values are lower than those from ACE-FTS, but agree within their uncertainty. Satellite measurements of O_3 and HNO_3 with higher measurement density could yield a spatially resolved OPE estimate.

5.2. Uncertainty in the OPE Estimate

[33] Here we examine sources of error in the ACE-FTS OPE estimate. The estimate is based on the assumption that the O_3 and HNO_3 concentrations in air exiting a convective updraft are constant throughout the tropics. In practice, higher O_3 concentrations in convective outflow can occur over polluted regions. We examine this issue using ACE-FTS CO measurements as a tracer for convective outflow of pollution. As the convective outflow from a cloud will have little HNO_3 due to wet deposition, the intercept of Figure 6 (O_3 = 25 ± 1 ppbv when HNO_3 = 0) is an estimate of the average O_3 concentration of the convective outflow. The intercept increases with increasing CO (Δintercept/ΔCO = 0.32 ± 0.04 ppbv O_3 per ppbv CO, r = 0.96) indicating that convective outflow in the tropical upper troposphere has higher O_3 concentrations over polluted regions. A similar relationship was found between CO concentrations and the intercept from PEM-Tropics measurements (Δintercept/ΔCO = 0.43 ± 0.02 ppbv O_3 per ppbv CO, r = 0.99).

[34] We estimate the OPE uncertainty due to the initial conditions of the convective outflow as the change in OPE due to a 1σ perturbation of CO. The OPE calculation decreases with increasing CO concentrations ($\Delta OPE/\Delta CO$ = −1.5 ± 0.1, r = −0.99), indicating that OPE is lower over regions with enhanced pollution outflow into the upper troposphere. An inverse relationship between CO and OPE is also found in calculations using measurements from PEM-Tropics ($\Delta OPE/\Delta CO$ = −2.9 ± 0.5, r = −0.94). This does not imply that OPE is inversely related to CO concentrations themselves, as CO is used here only as a tracer for pollution. Using the mean ACE-FTS tropical upper tropospheric CO (85 ± 23 ppbv) and the value of $\Delta OPE/\Delta CO$ we estimate that perturbing the initial CO conditions by one standard deviation would cause an OPE change of 33 mol/mol.

[35] In addition to errors from sensitivity to pollution outflow (δ_p = 33 mol/mol), the uncertainty of our OPE

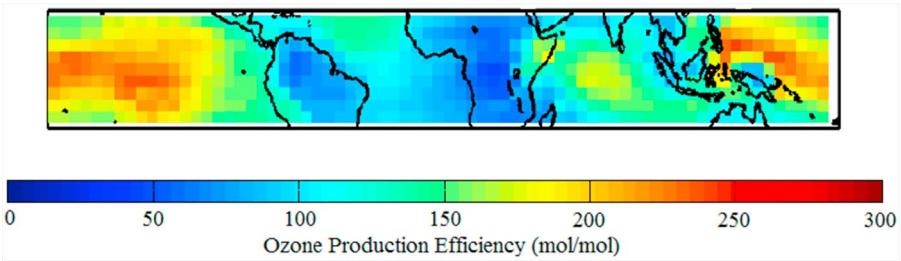

Figure 8. Simulated annual mean ozone production efficiency at 11 km, determined from GEOS-Chem simulated O_3 and HNO_3 production rates.

estimation contains contributions from the standard error of the reduced major axis regression (δ_r) as well as biases in the ACE-FTS measurements (δ_b). The standard error of the slope in Figure 6 as defined by *Miller and Kahn* [1962] is $\delta_r = 8$ mol/mol. The uncertainty due to ACE-FTS biases was calculated by reducing the O_3 and HNO_3 by their respective mean biases (assuming 12% bias for O_3, 15% bias for HNO_3) and recalculating OPE. As OPE is estimated by a ratio of O_3 and HNO_3 and the biases are of similar magnitude, the biases partly cancel resulting in an uncertainty of $\delta_b = 5$ mol/mol. Section 5.1 found that OPE estimated from the slope of O_3 and HNO_3 was biased high by 26%. Combining these errors in quadrature yields a combined global error of (+34, −61) mol/mol.

6. Conclusion

[36] This study evaluates OSIRIS O_3, ACE-FTS O_3, and ACE-FTS HNO_3 retrievals. Our focus was on the tropical troposphere, as these instruments had not been thoroughly evaluated in this region. Seasonal mean ozone profiles over eight regions were compared with measurements from the MOZAIC aircraft program and from ozonesondes. These regions were defined using the GEOS-Chem model to minimize sampling errors. Both satellite retrievals generally reproduce major ozone features in the upper troposphere such as summer enhancements at northern midlatitudes, and enhanced ozone concentrations over the tropical Atlantic versus the tropical Pacific. Annual mean O_3 concentrations in the upper troposphere from ACE-FTS are 10–13% higher than seasonal mean MOZAIC and ozonesonde profiles, while those from OSIRIS are higher by 5%. We indirectly evaluated ACE-FTS HNO_3 retrievals by comparing GEOS-Chem HNO_3 and NO_y concentrations with aircraft measurements and ACE-FTS. GEOS-Chem HNO_3 mixing ratios generally agreed with aircraft measurements above 12 km and were 9% lower than MOZAIC NO_y. Mean ACE-FTS measurements of HNO_3 are 29% higher on average than simulated values.

[37] Simultaneous measurements of HNO_3 and O_3 by ACE-FTS allowed for a calculation of an upper limit on the annual mean ozone production efficiency in the tropical troposphere. The ACE-FTS biases in O_3 and HNO_3 partially cancel in their ratio. A value of 196 (+34, −61) moles of O_3 produced per mole NO_x consumed was found and is consistent with the range of values seen in GEOS-Chem simulations. The ozone production efficiency of 249 (+21, −68) mol/mol inferred from ACE-FTS over the tropical Pacific is considerably larger than that of 146 (+16, −41) mol/mol over the tropical Atlantic, reflecting a decreased ozone production efficiency in a region where convective outflow is more polluted. Future improvement of satellite retrievals could yield a more refined estimate of the ozone production efficiency.

Appendix A: The GEOS-Chem Model

[38] The GEOS-Chem global 3-D chemical transport model [*Bey et al.*, 2001] is used in this study as a tool to aid comparisons between in situ and satellite comparisons. The simulation is driven by assimilated meteorological data from the Goddard Earth Observing System (GEOS) at the NASA Global Modeling and Assimilation Office (GMAO). Version 7-02-04 (http://geos-chem.org) is used here at 4° × 5° resolution with GEOS-4 meteorological fields for the year 2000. The tropical tropospheric ozone simulation for this version has been thoroughly evaluated by *Sauvage et al.* [2007b]. GEOS-4 data extend from the surface to 0.1 hPa including approximately 16 levels in the troposphere.

[39] The model includes a detailed simulation of tropospheric ozone-NO_x-hydrocarbon chemistry as well as of aerosols and their precursors. NO_x emissions from biomass burning, soils, lightning and anthropogenic sources included in the model have been recently described by *Sauvage et al.* [2007b]. The lightning parameterization is based on work by *Price and Rind* [1992] with vertical profiles from *Pickering et al.* [1998]. The lightning NO_x source is 5 Tg N/yr globally with 3 Tg occurring in the tropics between ±20° latitude. The spatial distribution of lightning is scaled to match the seasonal mean lightning flash rates as observed by the OTD and LIS satellite instruments [*Sauvage et al.*, 2007b]. HNO_3 scavenging by precipitation includes in-cloud and below-cloud scavenging by cloud droplets and ice crystals as described by *Jacob et al.* [2000].

[40] GEOS-Chem has been used in several recent studies to interpret tropospheric ozone measurements from satellite instruments such as TES [*Jourdain et al.*, 2007; *Bowman et al.*, 2008; *Zhang et al.*, 2008; *Nassar et al.*, 2009], OMI [*Martin et al.*, 2007; *Stajner et al.*, 2008; *Zhang et al.*, 2010], GOME [*Liu et al.*, 2006; *Sauvage et al.*, 2007a, 2007b], and TOMS and SAGE II [*Choi et al.*, 2008]. The O_3 simulation has been extensively evaluated against in situ measurements [*Jaeglé et al.*, 2003; *Hudman et al.*, 2004, 2007; *Li et al.*, 2004; *Auvray et al.*, 2007; *Sauvage et al.*, 2007b; *Zhang et al.*, 2008; *Nassar et al.* 2009].

[41] **Acknowledgments.** This research was supported by the Canadian Foundation for Climate and Atmospheric Science (CFCAS) and by the Canadian Space Agency (CSA). The ACE mission is funded primarily by the CSA and the Natural Sciences and Engineering Research Council of Canada (NSERC). Some funding was also provided by the UK Natural Environment Research Council (NERC). The authors acknowledge the strong support of the European Commission, Airbus, and the airlines (Lufthansa, Austrian, Air France) who have carried the MOZAIC equipment and performed maintenance free of charge since 1994. MOZAIC is presently funded by INSU-CNRS (France), Meteo-France, and Forschungszentrum (FZJ, Julich, Germany). The MOZAIC database is supported by ETHER (CNES and INSU-CNRS). Ozonesonde data available from WOUDC are provided by the India Meteorological Department (IMD), Japan Meteorological Agency (JMA), Hong Kong Observatory (HKO), University of Alabama at Huntsville (UAH), and the National Institute of Meteorology of Spain–Izana Observatory (INME-IZO).

References

Auvray, M., I. Bey, E. Llull, M. Schultz, and S. Rast (2007), A model investigation of tropospheric ozone chemical tendencies in long-range transported pollution plumes, *J. Geophys. Res.*, *112*, D05304, doi:10.1029/2006JD007137.

Bernath, P. F. (2006), Atmospheric Chemistry Experiment: Analytical chemistry from orbit, *Trends Analyt. Chem.*, *25*, 647–654, doi:10.1016/j.trac.2006.05.001.

Bernath, P. F., et al. (2005), Atmospheric Chemistry Experiment (ACE): Mission overview, *Geophys. Res. Lett.*, *32*, L15S01, doi:10.1029/2005GL022386.

Bey, I., D. J. Jacob, R. M. Yantosca, J. A. Logan, B. D. Field, A. M. Fiore, Q. Li, H. Liu, L. J. Mickley, and M. G. Schultz (2001), Global modeling of tropospheric chemistry with assimilated meteorology: Model description and evaluation, *J. Geophys. Res.*, *106*(D19), 23,073–23,095, doi:10.1029/2001JD000807.

Boone, C., and P. F. Bernath (2002), Pressure/temperature and volume mixing ratio retrievals for the Atmospheric Chemistry Experiment

(ACE), *Proc. SPIE Int. Soc. Opt. Eng.*, *4814*, 50–61, doi:10.1117/12.451526.

Bowman, K. W., D. Jones, J. Logan, H. Worden, F. Boersma, R. Chang, S. Kulawik, G. Osterman, and J. Worden (2008), Impact of surface emissions to the zonal variability of tropical tropospheric ozone and carbon monoxide for November 2004, *Atmos. Chem. Phys. Discuss.*, *8*, 1505–1548, doi:10.5194/acpd-8-1505-2008.

Choi, Y., Y. Wang, T. Zeng, D. Cunnold, E.-S. Yang, R. Martin, K. Chance, V. Thouret, and E. Edgerton (2008), Springtime transitions of NO_2, CO, and O_3 over North America: Model evaluation and analysis, *J. Geophys. Res.*, *113*, D20311, doi:10.1029/2007JD009632.

Degenstein, D. A., A. E. Bourassa, C. Z. Roth, and E. J. Llewellyn (2009), Limb scatter ozone retrieval from 10 to 60 km using a multiplicative algebraic reconstruction technique, *Atmos. Chem. Phys.*, *9*, 6521–6529, doi:10.5194/acp-9-6521-2009.

Dupuy, E., et al. (2009), Validation of ozone measurements from the Atmospheric Chemistry Experiment (ACE), *Atmos. Chem. Phys.*, *9*, 287–343, doi:10.5194/acp-9-287-2009.

Folkins, I., C. Braum, A. M. Thompson, and J. Witte (2002), Tropical ozone as an indicator of deep convection, *J. Geophys. Res.*, *107*(D13), 4184, doi:10.1029/2001JD001178.

Folkins, I., P. Bernath, C. Boone, L. J. Donner, A. Eldering, G. Lesins, R. V. Martin, B.-M. Sinnhuber, and K. Walker (2006), Testing convective parameterizations with tropical measurements of HNO_3, CO, H_2O, and O_3: Implications for the water vapor budget, *J. Geophys. Res.*, *111*, D23304, doi:10.1029/2006JD007325.

Hegglin, M. I., C. D. Boone, G. L. Manney, T. G. Shepherd, K. A. Walker, P. F. Bernath, W. H. Daffer, P. Hoor, and C. Schiller (2008), Validation of ACE-FTS satellite data in the upper troposphere/lower stratosphere (UTLS) using non-coincident measurements, *Atmos. Chem. Phys.*, *8*, 1483–1499, doi:10.5194/acp-8-1483-2008.

Hoell, J. M., D. D. Davis, D. J. Jacob, M. O. Rodgers, R. E. Newell, H. E. Fuelberg, R. J. McNeal, J. L. Raper, and R. J. Bendura (1999), Pacific Exploratory Mission in the tropical Pacific: PEM-Tropics A, August–September 1996, *J. Geophys. Res.*, *104*(D5), 5567–5583, doi:10.1029/1998JD100074.

Hoinka, K. P. (1998), Statistics of the Global Tropopause Pressure, *Mon. Weather Rev.*, *126*, 3303–3325, doi:10.1175/1520-0493(1998)126<3303:SOTGTP>2.0.CO;2.

Hudman, R. C., et al. (2004), Ozone production in transpacific Asian pollution plumes and implications for ozone air quality in California, *J. Geophys. Res.*, *109*, D23S10, doi:10.1029/2004JD004974.

Hudman, R. C., et al. (2007), Surface and lightning sources of nitrogen oxides over the United States: Magnitudes, chemical evolution, and outflow, *J. Geophys. Res.*, *112*, D12S05, doi:10.1029/2006JD007912.

Jacob, D. J., et al. (1996), Origin of ozone and NO_x in the tropical troposphere: A photochemical analysis of aircraft observations over the South Atlantic Basin, *J. Geophys. Res.*, *101*(D19), 24,235–24,250, doi:10.1029/96JD00336.

Jacob, D. J., H. Liu, C. Mari, and R. M. Yantosca (2000), Harvard wet deposition scheme for GMI, report, Harvard Univ. Atmos. Chem. Modeling Group, Cambridge, Mass.

Jaeglé, L., D. Jaffe, H. U. Price, P. Weiss-Penzias, P. I. Palmer, M. J. Evans, D. J. Jacob, and I. Bey (2003), Sources and Budgets for CO and O_3 in the northeastern Pacific during the spring of 2001: Results from the PHOBEA-II Experiment, *J. Geophys. Res.*, *108*(D20), 8802, doi:10.1029/2002JD003121.

Jourdain, L., S. S. Kulawik, H. M. Worden, K. E. Pickering, J. Worden, and A. M. Thompson (2007), Tropospheric vertical distribution of tropical Atlantic ozone observed by TES during the northern African biomass burning season, *Geophys. Res. Lett.*, *34*, L04810, doi:10.1029/2006GL028284.

Kalnay, E., et al. (1996), The NCEP/NCAR 40-year reanalysis project, *Bull. Am. Meteorol. Soc.*, *77*, 437–470, doi:10.1175/1520-0477(1996)077<0437:TNYRP>2.0.CO;2.

Kasibhatla, P. S., H. Levey II, and W. J. Moxim (1993), Global NO_x, HNO_3, PAN, and NO_y distributions from fossil fuel combustion emissions: A model study, *J. Geophys. Res.*, *98*(D4), 7165–7180, doi:10.1029/92JD02845.

Kleinman, L. I., P. H. Daum, D. G. Imre, J. H. Lee, Y.-N. Lee, L. J. Nennermacker, S. R. Springston, J. Weinstein-Lloyd, and L. Newman (2000), Ozone production in the New York City urban plume, *J. Geophys. Res.*, *105*(D11), 14,495–14,511, doi:10.1029/2000JD900011.

Kleinman, L. I., P. H. Daum, Y.-N. Lee, L. J. Nunnermacker, and S. R. Springston (2002), Ozone production efficiency in an urban area, *J. Geophys. Res.*, *107*(D23), 4733, doi:10.1029/2002JD002529.

Lacis, A. A., D. J. Wuebbles, and J. A. Logan (1990), Radiative forcing of climate by changes in the vertical distribution of ozone, *J. Geophys. Res.*, *95*(D7), 9971–9981, doi:10.1029/JD095iD07p09971.

Li, Q. B., D. J. Jacob, W. Munger, R. M. Yantosca, and D. D. Parrish (2004), Export of NO_y from the North American boundary layer: Reconciling aircraft observations and global model budgets, *J. Geophys. Res.*, *109*, D02313, doi:10.1029/2003JD004086.

Lin, X., M. Trainer, and S. C. Liu (1988), On the nonlinearity of the tropospheric ozone production, *J. Geophys. Res.*, *93*(D12), 15,879–15,888, doi:10.1029/JD093iD12p15879.

Liu, S. C., M. Trainer, F. C. Fehsenfeld, D. D. Parrish, E. J. Williams, D. W. Fahey, G. Hübler, and P. C. Murphy (1987), Ozone production in the rural troposphere and the implications for regional and global ozone distributions, *J. Geophys. Res.*, *92*(D4), 4191–4207, doi:10.1029/JD092iD04p04191.

Liu, X., et al. (2006), First directly retrieved global distribution of tropospheric column ozone from GOME: Comparison with the GEOS-Chem model, *J. Geophys. Res.*, *111*, D02308, doi:10.1029/2005JD006564.

Llewellyn, E. J., et al. (2004), The OSIRIS instrument on the Odin spacecraft, *Can. J. Phys.*, *82*, 411–422.

Logan, J. (1999), An analysis of ozonesonde data for the troposphere: Recommendations for testing 3-D models and development of a gridded climatology for tropospheric ozone, *J. Geophys. Res.*, *104*(D13), 16,115–16,149, doi:10.1029/1998JD100096.

Manney, G. L., et al. (2007), Solar occultation satellite data and derived meteorological products: Sampling issues and comparisons with Aura microwave limb sounder. *J. Geophys. Res.*, *112*, D24S50, doi:10.1029/2007JD008709.

Marenco, A., et al. (1998), Measurement of ozone and water vapor by Airbus in-service aircraft: The MOZAIC airborne program, An overview, *J. Geophys. Res.*, *103*(D19), 25,631–25,642, doi:10.1029/98JD00977.

Mari, C., D. J. Jacob, and P. Bechtold (2000), Transport and scavenging of soluble gases in a deep convective cloud, *J. Geophys. Res.*, *105*(D17), 22,255–22,267, doi:10.1029/2000JD900211.

Martin, R. V., et al. (2002), Interpretation of TOMS observations of tropical tropospheric ozone with a global model and in situ observations, *J. Geophys. Res.*, *107*(D18), 4351, doi:10.1029/2001JD001480.

Martin, R. V., B. Sauvage, I. Folkins, C. E. Sioris, C. Boone, P. Bernath, and J. Ziemke (2007), Space-based constraints on the production of nitric oxide by lightning, *J. Geophys. Res.*, *112*, D09309, doi:10.1029/2006JD007831.

McLinden, C. A., V. E. Fioletov, C. S. Haley, N. Lloyd, C. Roth, D. Degenstein, A. Bourassa, C. T. McElroy, and E. J. Llewellyn (2007), An evaluation of Odin/OSIRIS limb pointing and stratospheric ozone through comparisons with ozonesondes, *Can. J. Phys.*, *85*, 1125–1141.

Miller, R. L., and J. S. Kahn (1962), *Statistical Analysis in the Geological Sciences*, 205 pp., John Wiley and Sons, New York, New York.

Murphy, D. M., D. W. Fahey, M. H. Proffitt, S. C. Liu, K. R. Chan, C. S. Eubank, S. R. Kawa, and K. K. Kelly (1993), Reactive nitrogen and its correlation with ozone in the lower stratosphere and upper troposphere, *J. Geophys. Res.*, *98*(D5), 8751–8773, doi:10.1029/92JD00681.

Nassar, R., J. A. Logan, I. A. Megretskaia, L. T. Murray, L. Zhang, and D. B. A. Jones (2009), Analysis of tropical tropospheric ozone, carbon monoxide, and water vapor during the 2006 El Niño using TES observations and the GEOS-Chem model, *J. Geophys. Res.*, *114*, D17304, doi:10.1029/2009JD011760.

Petelina, S. V., et al. (2004), Comparison of the Odin/OSIRIS stratospheric ozone profiles with coincident POAM III and ozonesonde measurements, *Geophys. Res. Lett.*, *31*, L07104, doi:10.1029/2003GL019299.

Pickering, K. E., Y. S. Wang, W. K. Tao, C. Prince, and J. F. Muller (1998), Vertical distribution of lightning NO_x for use in regional and global chemical transport models, *J. Geophys. Res.*, *103*(D23), 31,203–31,216, doi:10.1029/98JD02651.

Popp, P. J., et al. (2009), Stratospheric correlation between nitric acid and ozone, *J. Geophys. Res.*, *114*, D03305, doi:10.1029/2008JD010875.

Price, C., and D. Rind (1992), A simple lightning parameterization for calculating global lightning distributions, *J. Geophys. Res.*, *97*(D9), 9919–9933, doi:10.1029/92JD00719.

Raper, J. L., M. M. Kleb, D. J. Jacob, D. D. Davis, R. E. Newell, H. E. Fuelberg, R. J. Bendura, J. M. Hoell, and R. J. McNeal (2001), Pacific Exploratory Mission in the Tropical Pacific: PEM-Tropics B, March–April 1999, *J. Geophys. Res.*, *106*(D23), 32,401–32,425, doi:10.1029/2000JD900833.

Ryerson, T. B., et al. (1998), Emissions lifetimes and ozone formation in power plant plumes, *J. Geophys. Res.*, *103*(D17), 22,569–22,583, doi:10.1029/98JD01620.

Sauvage, B., V. Thouret, A. M. Thompson, J. C. Witte, J.-P. Cammas, P. Nedelec, and G. Athier (2006), Enhanced view of the "Tropical Atlantic Ozone Paradox" and "Zonal Wave-one" from the in situ

MOZAIC and SHADOZ data, *J. Geophys. Res.*, *111*, D01301, doi:10.1029/2005JD006241.

Sauvage, B., R. V. Martin, A. van Donkelaar, and J. R. Ziemke (2007a), Quantification of the factors controlling tropical tropospheric ozone and the South Atlantic maximum, *J. Geophys. Res.*, *112*, D11309, doi:10.1029/2006JD008008.

Sauvage, B., R. V. Martin, A. van Donkelaar, X. Liu, K. Chance, L. Jaeglé, P. I. Palmer, S. Wu, and T.-M. Fu (2007b), Remote sensed and in situ constraints on processes affecting tropical tropospheric ozone, *Atmos. Chem. Phys.*, *7*, 815–838, doi:10.5194/acp-7-815-2007.

Stajner, I., et al. (2008), Assimilated ozone from EOS-Aura: Evaluation of the tropopause region and tropospheric columns, *J. Geophys. Res.*, *113*, D16S32, doi:10.1029/2007JD008863.

Thompson, A. M. (1992), The oxidizing capacity of the Earth's atmosphere: Probable past and future changes, *Science*, *256*, 1157–1165, doi:10.1126/science.256.5060.1157.

Thompson, A. M., K. E. Pickering, D. P. McNamara, M. R. Schoeberl, R. D. Hudson, J. H. Kim, E. V. Browell, V. W. J. H. Kirchhoff, and D. Nganga (1996), Where did tropospheric ozone over southern Africa and the tropical Atlantic come from in October 1992? Insights from TOMS, GTE TRACE A, and SAFARI 1992, *J. Geophys. Res.*, *101* (D19), 24,251–24,278, doi:10.1029/96JD01463.

Thompson, A. M., et al. (2003a), Southern Hemisphere Additional Ozonesondes (SHADOZ) 1998–2000 tropical ozone climatology: 1. Comparison with Total Ozone Mapping Spectrometer (TOMS) and ground-based measurements, *J. Geophys. Res.*, *108*(D2), 8238, doi:10.1029/2001JD000967.

Thompson, A. M., et al. (2003b), Southern Hemisphere Additional Ozonesondes (SHADOZ) 1998–2000 tropical ozone climatology: 2. Tropospheric variability and the zonal wave-one, *J. Geophys. Res.*, *108*(D2), 8241, doi:10.1029/2002JD002241.

Thouret, V., A. Marenco, P. Nédélec, and C. Grouhel (1998a), Ozone climatologies at 9–12 km altitude as seen by the MOZAIC airborne program between September 1994 and August 1996, *J. Geophys. Res.*, *103*(D19), 25,653–25,679, doi:10.1029/98JD01807.

Thouret, V., A. Marenco, J. Logan, P. Nédélec, and C. Grouhel (1998b), Comparisons of ozone measurements from the MOZAIC airborne program and the ozone sounding network at eight locations, *J. Geophys. Res.*, *103*(D19), 25,695–25,720, doi:10.1029/98JD02243.

Toon, O. B., et al. (2010), Planning, implementation, and first results of the Tropical Composition, Cloud and Climate Coupling Experiment (TC4), *J. Geophys. Res.*, *115*, D00J04, doi:10.1029/2009JD013073.

Trainer, M., et al. (1993), Correlation of ozone with NO_y in photochemically aged air, *J. Geophys. Res.*, *98*(D2), 2917–2925, doi:10.1029/92JD01910.

Volz-Thomas, A., M. Berg, T. Heil, N. Houben, A. Lerner, W. Petrick, D. Raak, and H.-W. Pätz (2005), Measurements of total odd nitrogen (NO_y) aboard MOZAIC in-service aircraft: Instrument design, operation and performance, *Atmos. Chem. Phys.*, *5*, 583–595, doi:10.5194/acp-5-583-2005.

von Savigny, C., I. C. McDade, E. Griffioen, C. S. Haley, C. E. Sioris, and E. J. Llewellyn (2005), Sensitivity studies and first validation of stratospheric ozone profile retrievals from Odin/OSIRIS observations of limb-scattered solar radiation, *Can. J. Phys.*, *83*, 957–972.

Wolff, M. A., et al. (2008), Validation of HNO_3, $ClONO_2$, and N_2O_5 from the Atmospheric Chemistry Experiment Fourier Transform Spectrometer (ACE-FTS), *Atmos. Chem. Phys.*, *8*, 3529–3562, doi:10.5194/acp-8-3529-2008.

Wu, S., L. J. Mickley, D. J. Jacob, J. A. Logan, R. M. Yantosca, and D. Rind (2007), Why are there large differences between models in global budgets of tropospheric ozone?, *J. Geophys. Res.*, *112*, D05302, doi:10.1029/2006JD007801.

Zhang, L., et al. (2008), Transpacific transport of ozone pollution and the effect of recent Asian emission increases on air quality in North America: An integrated analysis using satellite, aircraft, ozonesonde, and surface observations, *Atmos. Chem. Phys.*, *8*, 6117–6136, doi:10.5194/acp-8-6117-2008.

Zhang, L., D. J. Jacob, X. Liu, J. A. Logan, K. Chance, A. Eldering, and B. R. Bojkov (2010), Intercomparison methods for satellite measurements of atmospheric composition: Application to tropospheric ozone from TES and OMI, *Atmos. Chem. Phys. Discuss.*, *10*, 1417–1456, doi:10.5194/acpd-10-1417-2010.

P. F. Bernath, C. D. Boone, and K. A. Walker, Department of Chemistry, University of Waterloo, Waterloo, ON N2L 3G1, Canada.

M. Cooper and R. V. Martin, Department of Physics and Atmospheric Science, Dalhousie University, Halifax, NS B3H 3J5, Canada. (cooperm2@dal.ca)

D. A. Degenstein, Department of Physics and Engineering Physics, Institute of Space and Atmospheric Science, University of Saskatchewan, Saskatoon, SK S7N 5E2, Canada.

C. A. McLinden, Environment Canada, Toronto, ON M2H 5T4, Canada.

B. Sauvage, Laboratoire d'Aérologie, CNRS, Université de Toulouse III, F-31062 Toulouse, France.

A. Volz-Thomas, Institut für Energie und Klimaforschung 8: Troposphäre, Forschungszentrum Jülich, DE-52425 Jülich, Germany.

C. Wespes, Spectroscopie de l'Atmosphère, Chimie Quantique et Photophysique, Université Libre de Bruxelles, B-1050 Brussels, Belgium.